ELSEVIER

Ceramics International 29 (2003) 897–905

CERAMICS INTERNATIONAL

www.elsevier.com/locate/ceramint

Effect of β-Si_3N_4 seed particles on the property of sintered reaction-bonded silicon nitride

Joo-Sin Lee[a,*], Ji-Hun Mun[a], Byung-Dong Han[b], Hai-Doo Kim[b]

[a]*Department of Materials Science and Engineering, Kyungsung University, Pusan 608-736, South Korea*
[b]*Ceramic Materials Group, Korea Institute of Machinery and Materials, Changwon, Kyungnam 641-010, South Korea*

Received 30 September 2002; received in revised form 18 October 2002; accepted 7 December 2002

Abstract

The effect of seeding on the microstructural development and mechanical properties of sintered reaction-bonded silicon nitride was investigated by the use of β-Si_3N_4 particles. Seeding of an appropriate amount of the β-Si_3N_4 particles gave rise to the promotion of density and the resulting increase in fracture strength and hardness. The fracture toughness was also increased due to the development of elongated grains. On the other hand, addition of a large amount of seed particles showed lower strength and fracture toughness owing to the coalescence of large elongated grains. By seeding of 2 wt.% β-Si_3N_4 particles on Si powders of 7 μm, high fracture strength of 1100 MPa and fracture toughness of 7.2 MPa·$m^{1/2}$ were obtained in sintered reaction-bonded silicon nitride ceramics.

Keywords: Powders-gas phase reaction; Elongated grain; Mechanical properties; Sintered reaction-bonded silicon nitride; β-Si_3N_4 Seed

1. Introduction

Silicon nitride is one of the most promising ceramic materials for use in gas turbine engines and other high-temperature structural applications because of its high-temperature strength, thermal shock resistance, chemical stability and excellent creep resistance [1].

There are three kinds of silicon nitride ceramics: hot-pressed Si_3N_4, sintered Si_3N_4 and reaction-bonded Si_3N_4. Among these, reaction-bonded silicon nitride (RBSN) offers a number of advantages over materials produced by more conventional processes such as hot-pressing and sintering. In particular, complex shapes can be formed to meet precise dimensional tolerances with minimal or in some cases no machining. Also, RBSN produced by reaction-bonding of silicon powder compacts is economical compared to sintered Si_3N_4 because the price of Si powder is much lower than that of Si_3N_4 powder. Reaction-bonded processes generally require lower fabrication temperatures than hot-pressing and sintering, and it is favorable for processing ceramic-matrix composites where high temperatures can damage the reinforcement phase. However, the mechanical properties of RBSN are not enough for advanced engineering applications. Although sintered RBSN (SRBSN) has been fabricated to improve the mechanical properties, the fracture toughness of SRBSN sometimes cannot meet the high reliability and performance specifications required for advanced engineering applications. Therefore, it is important to make further improvements in the fracture toughness of this material.

Silicon nitride ceramics can have a high fracture toughness by developing "in situ composities" or "self-reinforced" microstructures, which are composed of fine matrix grains and some large elongated grains [2–5]. The increase of fracture toughness has been attributed to the large elongated grains which favor crack deflection and/or crack bridging [6–8].

Typical silicon nitride ceramics fabricated by pressureless sintering using Si_3N_4 raw powders have a fracture toughness in the range of 4–6 MPa·$m^{1/2}$. During the pressureless sintering process, α-Si_3N_4 grains dissolve in the liquid phase and precipitate as the rod-like β grains with a length of several μm. However, when Si_3N_4 powder is sintered using a gas-pressure sintering

* Corresponding author. Tel.: +82-51-620-4763; fax: +82-51-622-8452.
E-mail address: leejs@star.kyungsung.ac.kr (J.-S. Lee).

0272-8842/03/$30.00
doi:10.1016/S0272-8842(03)00034-8

technique, the large elongated grains with a high aspect ratio and several tens of μm in length develop within a small-grained matrix. These materials are called "in situ composites" or "self-reinforced materials", and present a bimodal microstructure. These materials have a fracture toughness as high as 8–11 $MPa{\cdot}m^{1/2}$ [2–5].

However, most often the existence of larger elongated grains leads to a decrease in fracture stength due to the increase in defects. Therefore, in order to improve the fracture toughness without exerting a harmful influence on other mechanical properties, proper control of the development of elongated grains within the silicon nitride matrix becomes a decisive step. As one way to control the development of elongated grains, β-seed addition on starting powders is introduced.

For the increase of fracture toughness by β-seed addition, studies have been mostly performed on the addition on Si_3N_4 powders [9–12]. The fracture toughness and strength were substantially improved by controlling the content and size distribution of β-seeds. Hirao et al. [9] reported that by seeding morphologically regulated rod-like β-Si_3N_4 single crystal particles, the fracture toughness was improved from 6.3 to 8.4–8.7 $MPa{\cdot}m^{1/2}$, retaining high strength of about 1 GPa. However, only limited studies were reported on the β-seed addition on Si powders, used as raw-material in fabricating RBSN [13].

In this work, the effect of seeding on the microstructural development and mechanical properties of sintered reaction-bonded silicon nitride is investigated by the use of β-Si_3N_4 particles. The effect on Si powders with different particle sizes is investigated also.

2. Experimental procedure

The Si powders (Permascand) used for this study were coarse powder ($d_{50}=7\mu m$, BET surface area of 1.2 m^2/g) and fine powder ($d_{50}=2\mu m$, BET surface area of 6.0 m^2/g). According to the manufacturer's information, both powders contained impurities of 0.07 wt.% Fe, 0.07 wt.% Al, 0.01 wt.% Ca, 0.1 wt.% C and 0.2–1.0 wt.% O (oxygen content is dependent on the particle size distribution). The oxygen contents measured by the oxygen/nitrogen analyzer (LECO) were 0.56 and 1.9 wt.% for the average particle sizes of 7 and 2 μm, respectively. The average particle size was confirmed by Coulter LS particle size analyzer and Hitachi S-2400 scanning electron microscope.

The β-Si_3N_4 particles (Denki Kagaku) used as seed were prepared by separating the particles of $d_{50}=1$ μm from the $d_{50}=2$ μm powder provided by the supplier. To separate the seed particles the sedimentation method and the centrifugal separation method were used together. Fig. 1 shows the SEM micrograph of β-Si_3N_4 seed particles having a size of approximately 1 μm, and its particle size distribution with $d_{50}=1$ μm is also shown in Fig. 2. The amount of added seed particles were 0, 2, 5 and 10 wt.%. Y_2O_3 (H.C.Starck, fine grade) and Al_2O_3 (Sumitomo Chemical AKP-30) were also used as sintering aids. Addition contents of the sintering aids were 6 wt.%Y_2O_3 and 1 wt.%Al_2O_3.

Fig. 3 shows the schematic flow diagram of experimental procedures. Si powders with sintering aids and 1 wt.% PEG 300 as binder were mixed for 12 h in a plastic jar with Si_3N_4 balls in ethanol. The mixed powders with β-Si_3N_4 seed particles were remixed for 3 h. They were dried at 40–50 °C on a hot plate while stirring. The dried powder mixture were sieved to −80–+140 mesh, and pressed uniaxially into the disk-shaped compacts of 30 mm dia. under 50 MPa. After compaction, the PEG 300 binder was burnt out to enhance the pore-channel distribution in the green compacts. The burn-out process was done at 600 °C for 1 h under a flowing N_2 atmosphere.

After the binder burn-out operation, the compacts were subjected to nitridation in a tube furnace with a

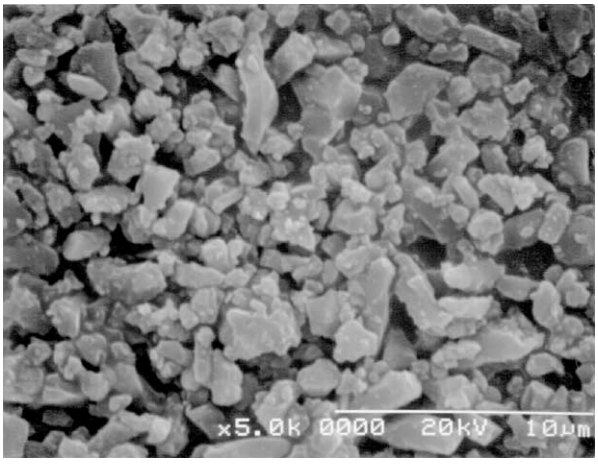

Fig. 1. SEM micrograph of β-Si_3N_4 seed particles.

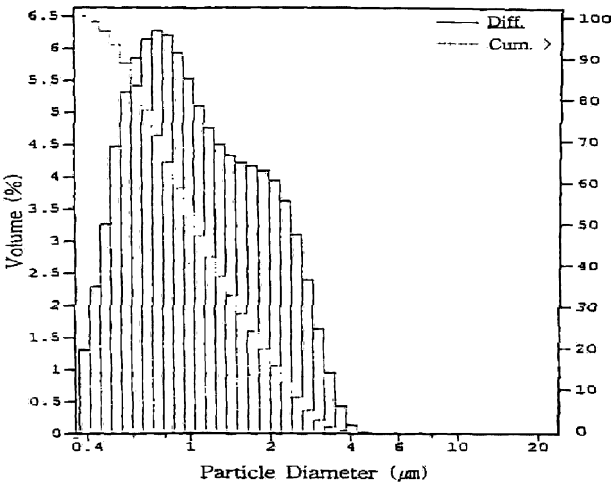

Fig. 2. Particle size distribution of β-Si_3N_4 seed particles.

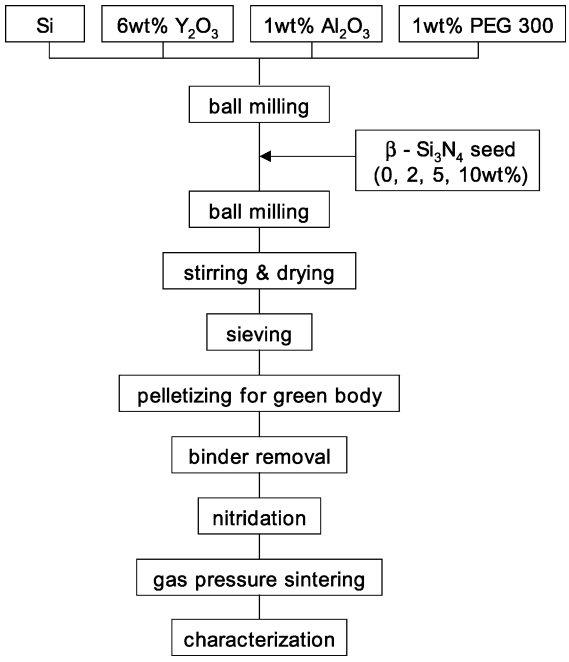

Fig. 3. Schematic flow diagram of experimental procedures.

quasi-static 95%N_2/5%H_2 gas mixture, controlled at a positive pressure of 20 KPa. It is essentially a gas demanding system wherein the temperature is regulated by a signal from a pressure transducer. As the nitriding reaction proceeds, nitrogen is consumed and the furnace pressure drops below the control pressure. The gas mixture is then allowed to enter the furnace to maintain the constant control pressure of 120 KPa. Simultaneously, temperature is held for a minimum time to allow the reaction to approach equilibrium. The nitridation was done as the multi-step process up to 1450 °C during 29.5 h. The holding time at the maximum nitridation temperature of 1450 °C was 2 h.

After the nitridation process the percentage of nitridation and the relative density were measured. The percentage of nitridation was calculated from the weight change before and after nitridation. The relative density was calculated from the theoretical density and the sintered density obtained from the weight and dimension measurement.

Postsintering was performed in gas-pressure-sintering furnace (Ionex, USA) under different N_2 gas pressures. The postsintering was performed at 1850, 1900 and 1950 °C for 3 h under 2 MPa N_2 pressure.

X-ray diffraction (XRD) technique was employed to identify the phases and to do the quantitative phase analysis. XRD was done on the cross section and on the surface of the sintered specimens by using Rigaku D/MAX 2200 diffractometer. To perform the quantitative phase analysis of α-Si_3N_4, β-Si_3N_4 and Si, X-ray diffraction analysis suggested by Jovanovic et al. [14] was used.

The fracture strength was measured on the bar samples 3×4×25 mm in a three-point bending fixture with a span of 20 mm and a crosshead speed of 0.5 mm/min (Instron 2406). The surfaces of the bars were machined and then polished with diamond paste down to 1 μm. The fracture toughness was measured on the polished surfaces by the indentation crack length method using 20 N load in a Vickers hardness tester (Mitutoyo AVK-C2).

For microstructural investigation, the cross section of the polished specimens was plasma-etched using a gas mixture of 95% CF_4 and 5% O_2 for 4 min. The samples were then Au-coated and examined with scanning electron microscope (SEM).

3. Results and discussion

The percentage of nitridation for the specimens reaction-sintered with coarse powder and fine powder was measured as a function of the β-Si_3N_4 seed content. An average of 5 specimens was taken. The specimens using coarse powder showed 92–95% nitridation, while the specimens using fine powder showed 88–90% nitridation, depending on the β-Si_3N_4 content. The results show that the nitridation rate increases apparently with increasing particle size. The variation with β-seed addition, however, was not shown.

The increase in the nitridation rate with increasing particle size is probably due to the decrease in SiO_2 content on the starting Si powders. The oxygen contents measured by the oxygen/nitrogen analyzer were 1.9 and 0.56 wt.% for the average particle sizes of 2 and 7 μm, respectively. The amount of SiO_2 converted from these oxygen contents is 3.56 and 1.05 wt.%, respectively. Thus, in the specimens using coarse powder the small amount of liquid phase is formed, and there is a less possibility of a blocking of pore-channel structures. The existence of the continuous pore-channel structures in the nitridation process improves the diffusion of N_2 gas, and then enhances a nitridation rate. Thus, the enhanced nitridation rate is expected in the specimens using coarse powder, which seems to be due to smaller amount of liquid phase and large pore-channel structures in the compacts.

XRD measurement was performed on the cross section and on the surface of the reaction-sintered specimens. All patterns had the peaks due to α- and β-Si_3N_4 as the major phases. However, the distinct difference in the second phase was shown. It was noticeable that the specimens using fine powder and coarse powder showed the appearance of α-$Y_2Si_2O_7$ phase and $Y_{10}Si_6O_{24}N_2$ phase, respectively. Each second phase appeared on all XRD patterns measured as a function of the β-seed content. Exception was given on the XRD pattern measured on the sample surface in the case of 10 wt.%

β-seed addition on coarse powder. The peaks due to α-$Y_2Si_2O_7$ phase additionally appeared in that case. In the case of fine powder the peaks due to α-$Y_2Si_2O_7$ phase strongly existed on all XRD patterns, but the peaks due to $Y_{10}Si_6O_{24}N_2$ phase weakly existed also.

We also calculated the volume fractions of β-Si_3N_4 on the cross section and on the surface of the specimens. The data showed that relatively large amounts of β-phases are formed on the surface rather than in the inside. The increase in β-phase content with increasing β-seed content was also shown.

Pseudoquaternary phase equilibrium diagram for the system Si–Y–O–N was reported by Gauckler et al. [15]. As shown in their figure, if yttrium content (x-axis) is fixed, Si_3N_4 phase is compatible with $Y_2Si_2O_7$ phase, $Y_{10}Si_6O_{24}N_2$ phase and $YSiO_2N$ phase with decreasing oxygen content. This supports a fact that in the case of fine 2 μm powders containing more SiO_2 content $Y_2Si_2O_7$ phase dominantly appears as the second phase, and $Y_{10}Si_6O_{24}N_2$ phase dominantly appears in 7 μm powders containing less SiO_2 content. And also, $YSiO_2N$ phase appeared in another experiments [16] using more coarse 25 μm powders containing much less SiO_2 content. These facts are consistent with the variation in the second phase depending on particle size. For details, it is discussed elsewhere [16]. At this point eq. Y% has a somewhat higher value in fine powders, but it is approximately calculated to be 1.8–1.85 eq.%. Increasing oxygen content of the Si powder favors the formation of second phases with low Y/O ratio.

The formation of relatively large amounts of β-phases was observed on the surface, as mentioned above. This implies that there is more oxygen content on the surface of the specimens. This result is supported by a fact that in the case of coarse powder α-$Y_2Si_2O_7$ phase, which appears under the existence of more oxygen content, is formed on the surface only. A fact that α-$Y_2Si_2O_7$ phase is formed in 10 wt.% seed addition only, supports this also. The composition ratio of Si and β-Si_3N_4 to Al_2O_3 and Y_2O_3 in the raw powder mixture is the largest in 10 wt.% addition. Raw-Si powders and β-Si_3N_4 seed particles contain the native oxide SiO_2 layers.

The increase in β-phases with increasing β-seed content implies that β-seed influences on the α→β phase transformation. The transformation of α to β is explained by the dissolution of α-particles and its reprecipitation onto the β-phase. The observation of an

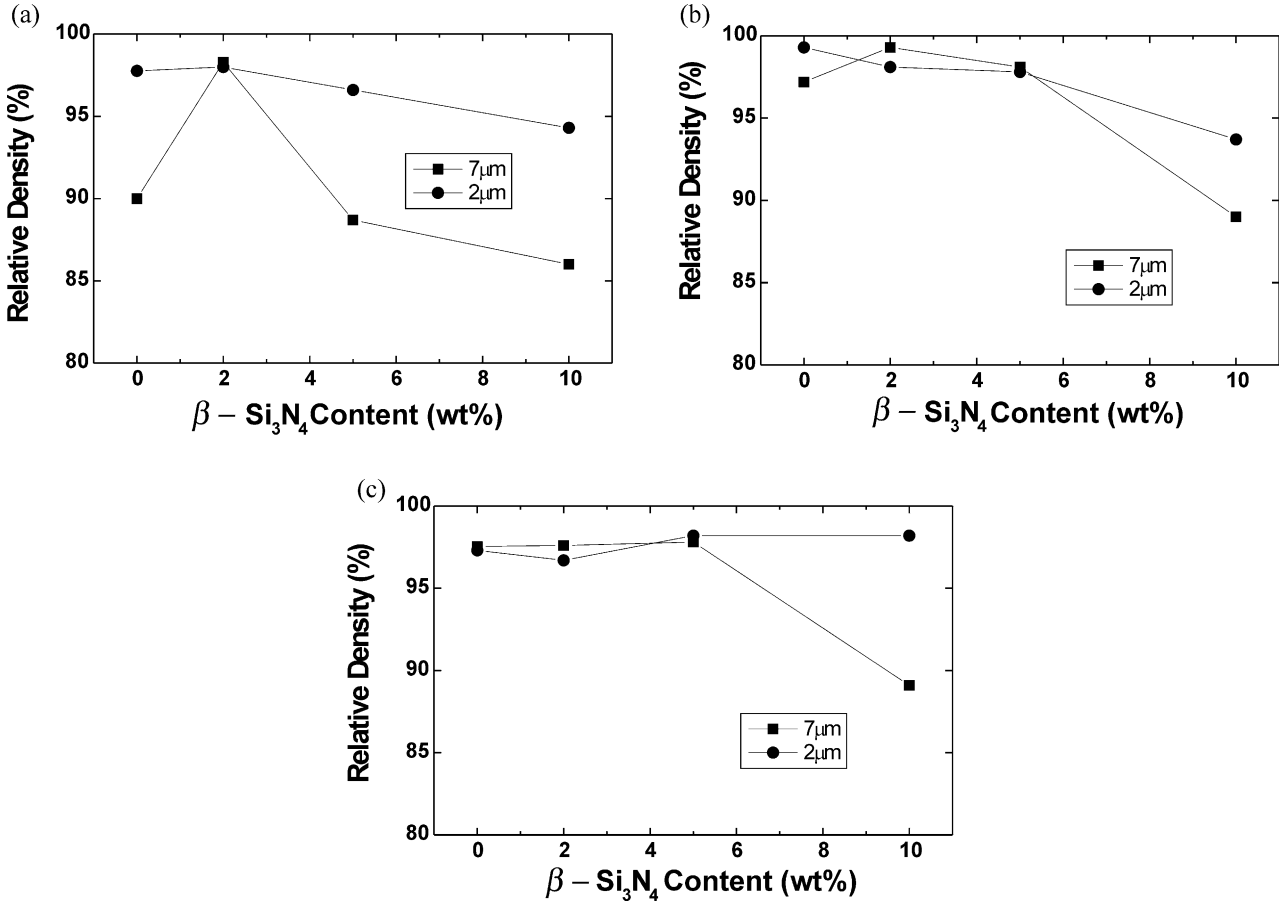

Fig. 4. Relative density versus β-Si_3N_4 content for the specimens gas-pressure-sintered at different temperatures. (a) 1850 °C, (b) 1900 °C and (c) 1950 °C.

increase in β-phases with increasing β-seed content suggests a decrease in activation energy for the reprecipitation of β-phase on β-seeds. Lu et al. [12] reported that a core/shell structure was observed in large elongated β-Si_3N_4 grain of seeded specimens. They also reported that as a result of the elemental analysis of the core and shell, the elemental compositions in the core were close to those of the β-seeds. They suggest that the core is probably a β-seed, which acts as a nucleus during liquid-phase sintering.

Fig. 4 shows the relative densities of the specimens gas-pressure-sintered at different sintering temperatures. The specimens using fine powder exhibit relatively higher densification, and a decline in density is shown in addition of a large amount of seed particles. The density difference between fine powder and coarse powder becomes small with increasing sintering temperature. In the variation of addition the higher density is obtained on 2 wt.% β-seed addition.

The fracture strengths of the specimens gas-pressure-sintered at different temperatures are shown in Fig. 5. The left side is for the specimens using fine powder, and the right side is for coarse powder. At 1850 °C as shown in Fig. 5(a), the relatively higher values of fracture strength are shown in the specimens using fine powder rather than coarse powder, reflecting the density variation of Fig. 4. However, as the sintering temperature is increased the strength difference between the two powders becomes small, as shown in Fig. 5(b) and (c). The effect of seeding is shown also. The increased strength is shown in a little addition, while the strength is decreased with increasing the additive amount exceeding an appropriate amount. The variation of Vickers microhardness was measured also. The observed variation in hardness was a direct consequence of the variation in strength and density.

Fig. 6 shows the fracture toughness of the gas-pressure-sintered specimens. A different behavior from Fig. 5 is observed. The fracture toughness is increased with increasing particle size. The effect of seeding is shown also. When the amount of additive becomes larger, a declining tendency in toughness is shown.

Fig. 7 shows the SEM micrographs of the specimens gas-pressure-sintered at 1850 °C with fine powder. Numeral letters in the middle of the micrographs such as 0, 2 and 5 represent an addition wt.% of β-seed. Numeral letters below micrographs such as 1000 and 5000 represent a magnifying power. The SEM micrographs show the dense-structure reflecting the high densification of 97–98% TD and the development of elongated grains. In particular, the development of large elongated grains is shown with increasing β-seed

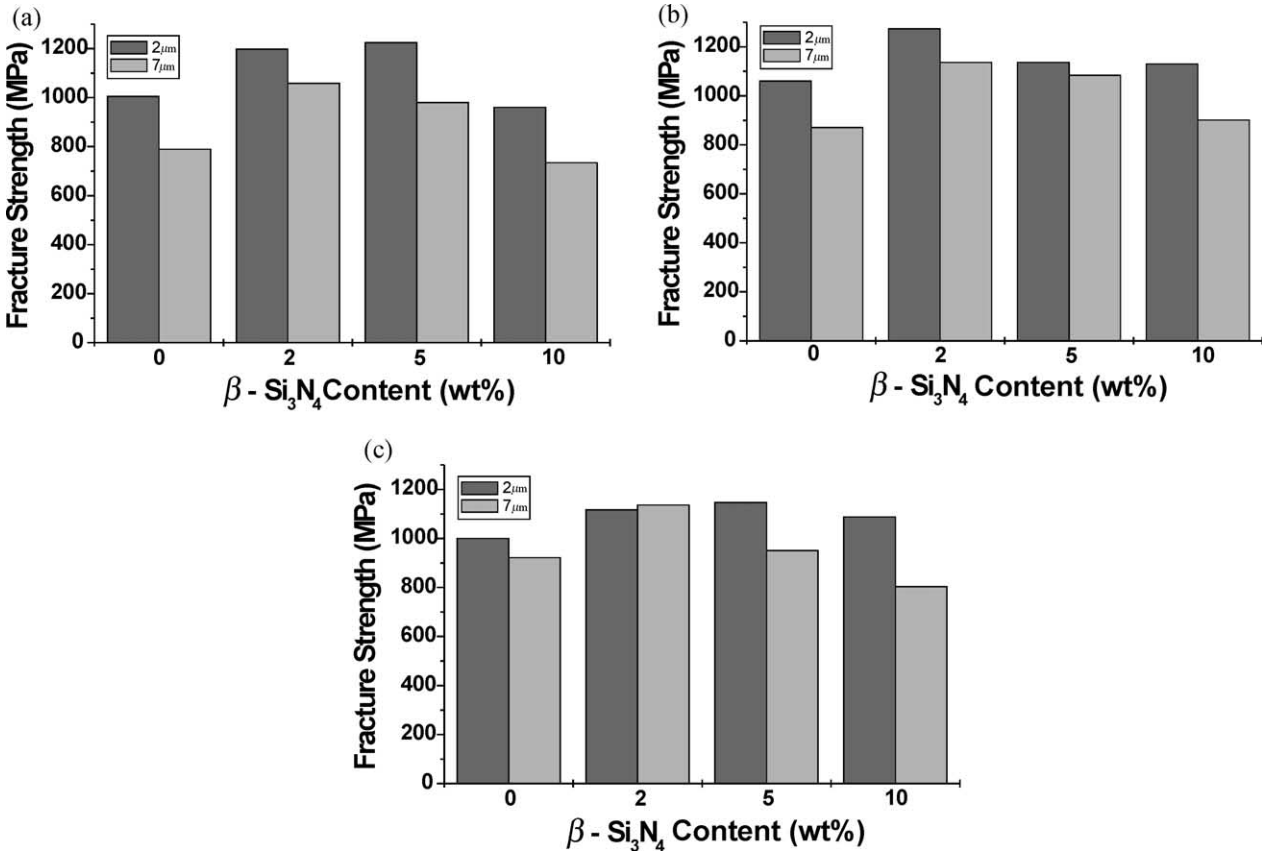

Fig. 5. Fracture strength versus β-Si_3N_4 content for the specimens gas-pressure-sintered at different temperatures. (a) 1850 °C, (b) 1900 °C and (c) 1950 °C.

content. As the sintering temperature is increased to 1900 and 1950 °C, the large elongated grains developed much more.

In the case of coarse powder, the development of larger elongated grains was remarkably shown more than in fine powder. Such a development of elongated grains explains well a situation in which the high values of toughness are obtained in coarse powder. Fig. 8 shows the SEM micrographs of the specimens gas-pressure-sintered at 1900 °C with coarse powder. The development of elongated grains is more remarkable than Fig. 7 of fine powder, though the temperature is different. A tendency hindering the growth of larger elongated grains owing to the coalescence of larger grains is seen on 5 wt.% addition of β-seed.

We studied in another work the effect of raw-Si particle size on microstructure and mechanical properties of sintered reaction-bonded silicon nitride [16]. According to the work, the powder size exerts a great influence on the microstructural development, because of the difference in the amount and in distribution of liquid phase due to the difference in the native oxide SiO_2 content. In this case using coarse powder, the decrease in density and the increase in toughness were shown as a result of the development of large elongated grains owing to the insufficiency and the inhomogeneous distribution in liquid phase contents. In the case using fine powder, however, the increase in density and strength was shown because of the appropriate amount and the good spread of liquid phase.

The effect of seed addition is also notable. The seeding of an appropriate amount of β-Si_3N_4 particles give rise to the promotion of density and the resulting increase in fracture strength and hardness. The fracture toughness is also increased due to the development of elongated grains. On the other hand, addition of a large amount of seed particles leads to the decrease in fracture strength and fracture toughness owing to the coalescence of large elongated grains.

For the promotion in density with adding a little amount of β-seed, Lee et al. [13] attributed the increase in the nitridation rate to the promotion in the pore-channel structures. They used a β-seed larger than the size of the starting Si powder. However, the variation in the nitridation rate with β-seed addition was not shown in this study, and a definite explanation has not been accomplished. The promotion in density and the resulting increase in strength and hardness, however, were shown.

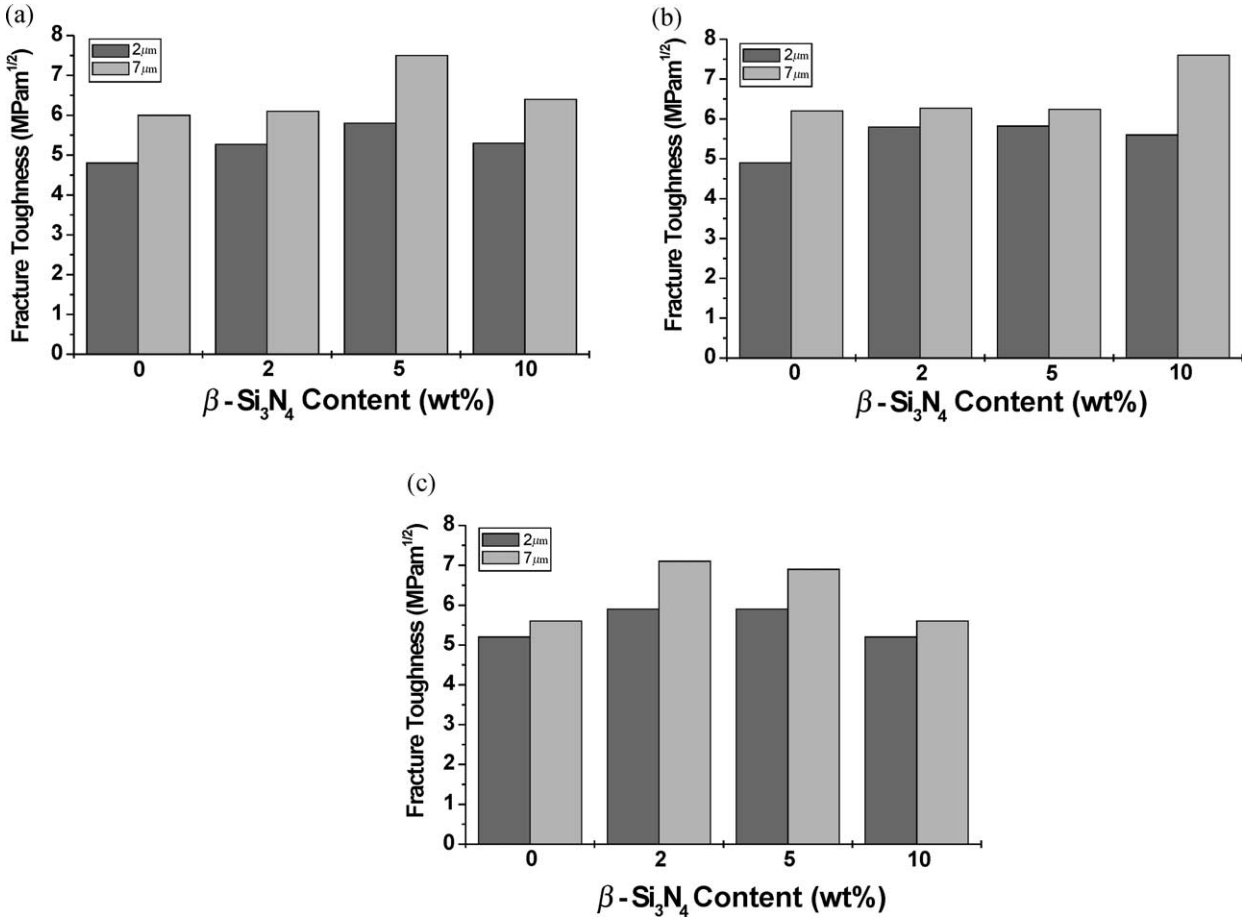

Fig. 6. Fracture toughness versus β-Si_3N_4 content for the specimens gas-pressure-sintered at different temperatures. (a) 1850 °C, (b) 1900 °C and (c) 1950 °C.

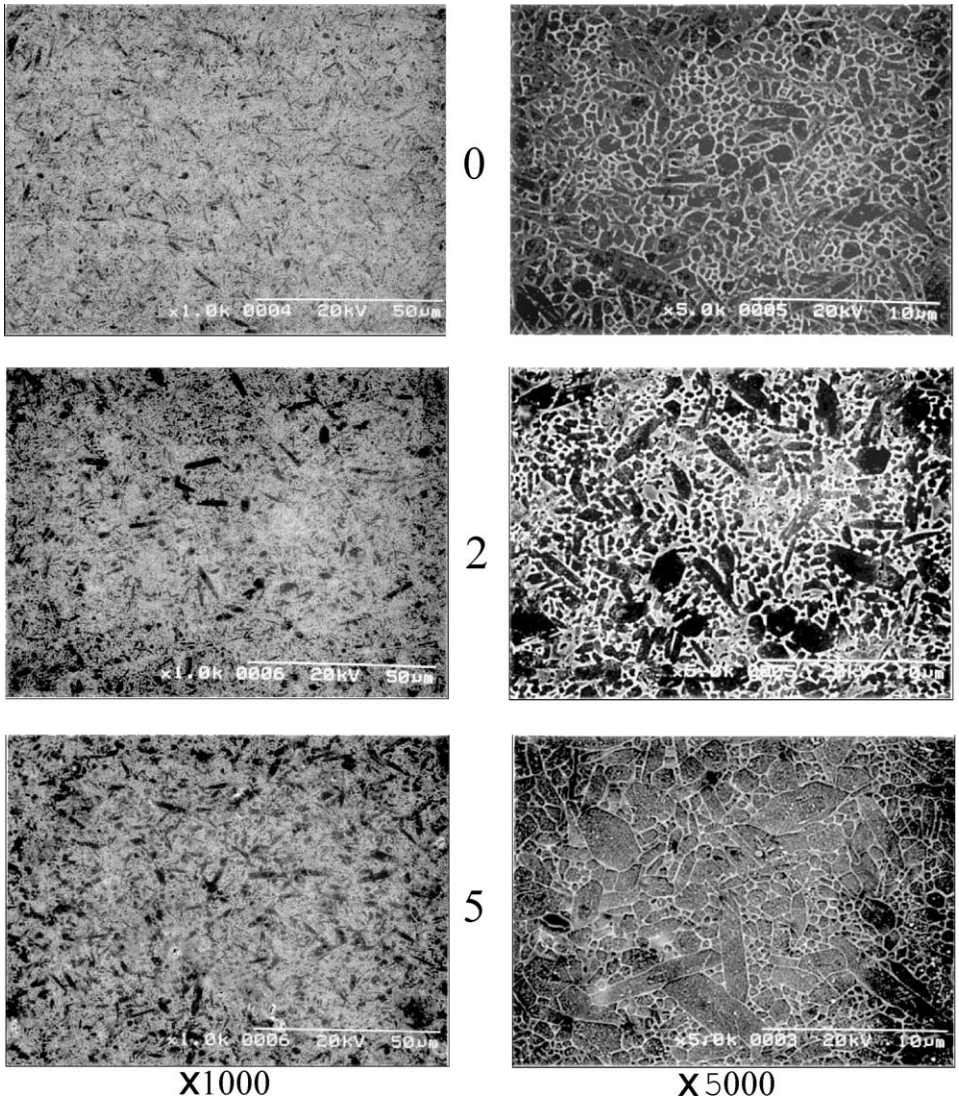

Fig. 7. SEM micrographs of the specimens gas-pressure-sintered at 1850 °C with fine powder.

As the β-seed is added, the large elongated grains with a high aspect ratio, which are grown from the β-seed crystal, exist in large quantities, and the toughness becomes larger owing to the toughening mechanism such as crack deflection [6] and crack bridging [7]. However, as the additive amount exceeds an appropriate amount, the decrease in density due to the large elongated grains grown from place to place and the decrease in toughness due to the coalescence and the breakdown of large elongated grains occurred. In fact, as shown in Fig. 8 the large elongated grains promoted up to 2 wt.% addition break down on 5 wt.% addition.

The SEM photographs also show a core/shell structure, for which β-seed acts as a growing site of β-Si_3N_4 grains. As the β-seed is added with an appropriate amount, the resulting growth in β-Si_3N_4 grains is shown, and it is effective. In this study, the increase in strength and toughness is shown in the case of 2 wt.% β-seed addition.

4. Conclusions

The effect of seeding on the property of sintered reaction-bonded silicon nitride was studied by the addition of β-Si_3N_4 seed particles on the starting Si powders with different particle sizes. As a result of the investigation on the nitridation behavior, the densification behavior and the microstructural development during postsintering, and the resulting mechanical properties of the sintered material, the following conclusions can be drawn.

In the nitridation at 1450 °C, the effect of seed addition was not shown. β-Phase, however, was increased with increasing β-seed content. The higher nitridation

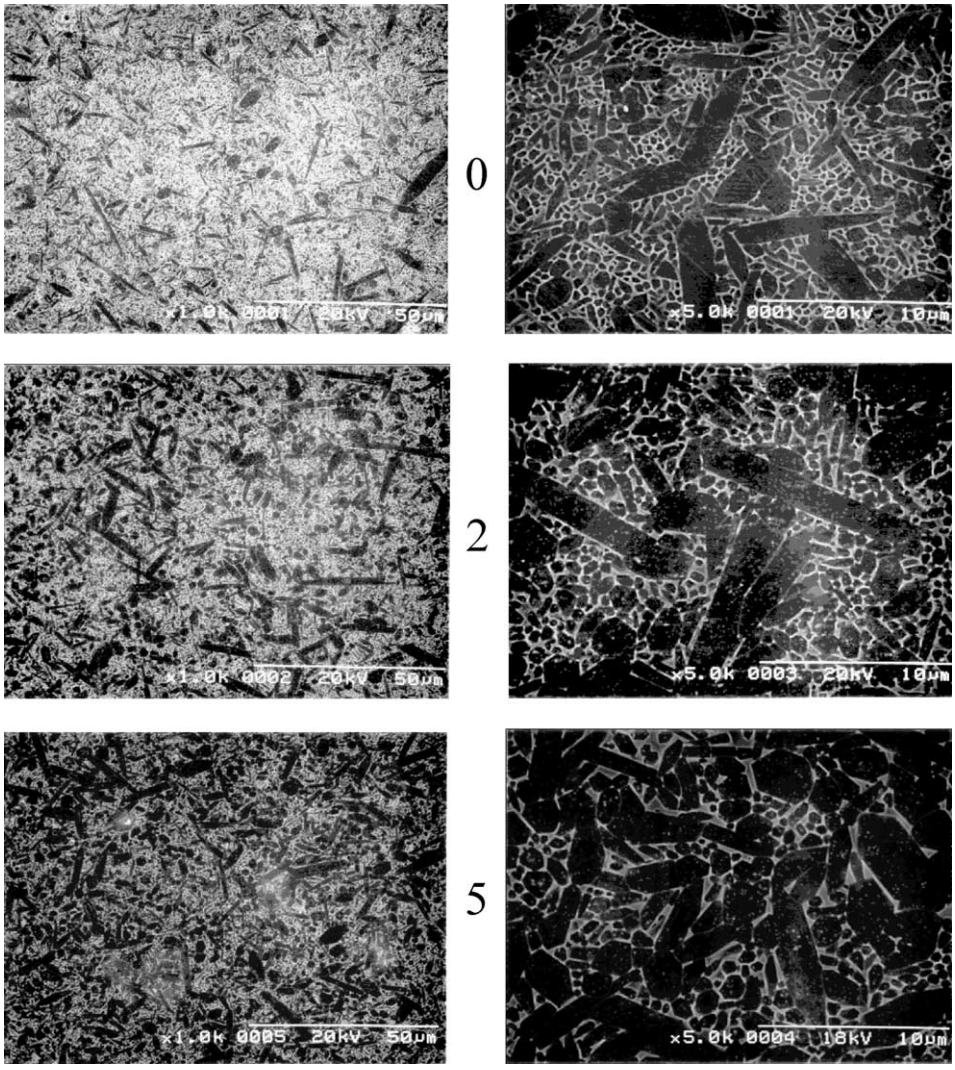

Fig. 8. SEM micrographs of the specimens gas-pressure-sintered at 1900 °C with coarse powder.

rate was obtained in the specimens using coarse powder, regardless of the variation in β-seed content, due to the decrease in SiO_2 content on the starting Si powders.

In the gas-pressure sintering of high temperatures, β-seed addition of an appropriate amount gave rise to the promotion of density and the resulting increase in fracture strength and hardness. The fracture toughness was also increased due to the development of elongated grains. On the other hand, addition of a large amount led to the decrease in density due to the large elongated grains grown from place to place, the resulting decrease in fracture strength, and the decrease of fracture toughness due to the coalescence of large elongated grains. The optimum amount of β-seed addition seemed to be 2 wt.%. Higher values of fracture toughness were obtained in the specimens using coarse powder, due to the fast growth of large elongated grains. By seeding of 2 wt.% β-Si_3N_4 particles on Si powders of 7 μm, high fracture strength of 1100 MPa and fracture toughness of 7.2 MPa·$m^{1/2}$ were obtained in sintered reaction-bonded silicon nitride ceramics.

Acknowledgements

This article was financially supported by the RCEC of Dongeui University.

References

[1] L.J. Schioler, Heat engine ceramics, Am. Ceram. Soc. Bull. 64 (2) (1985) 268–294.
[2] E. Tani, S. Umebayashi, K. Kishi, K. Kobayashi, M. Nishijima, Gas-pressure sintering of Si_3N_4 with concurrent addition of Al_2O_3 and 5 wt.% rare-earth oxide: high fracture toughness Si_3N_4 with fiber-like structure, Am. Ceram. Soc. Bull. 65 (9) (1986) 1311–1315.
[3] C.W. Li, J. Yamanis, Super-tough silicon nitride with R-curve behavior, Ceram. Eng. Sci. Proc. 10 (7–8) (1989) 632–645.

[4] T. Kawashima, H. Okamoto, H. Yamamoto, A. Kitamura, Grain size dependence of the fracture toughness of silicon nitride ceramics, J. Ceram. Soc. Jpn 99 (4) (1991) 320–323.
[5] N. Hirosaki, Y. Akimune, M. Mitomo, Effect of grain growth of β-silicon nitride on strength, Weibull modulus and fracture toughness, J. Am. Ceram. Soc. 76 (7) (1993) 1892–1894.
[6] K.T. Faber, A.G. Evans, Crack deflection process, Acta Metall. 31 (4) (1983) 565–584.
[7] P.F. Becher, C.H. Hsueh, P. Angelini, T.N. Tiegs, Toughening behavior in whisker-reinforced ceramic matrix composites, J. Am. Ceram. Soc. 71 (12) (1988) 1050–1061.
[8] P.F. Becher, Microstructural design of toughened ceramics, J. Am. Ceram. Soc. 74 (2) (1991) 255–269.
[9] K. Hirao, T. Nagaoka, M.E. Brito, S. Kanzaki, Microstructure control of silicon nitride by seeding with rodlike β-silicon nitride particles, J. Am. Ceram. Soc. 77 (7) (1994) 1857–1862.
[10] K. Hirao, T. Nagaoka, M.E. Brito, S. Kanzaki, Mechanical properties of silicon nitrides with tailored microstructure by seeding, J. Ceram. Soc. Jpn 104 (1) (1996) 54–58.
[11] T. Hirano, J. Yang, K. Niihara, Effect of seed crystal properties on the microstructure of Si_3N_4 ceramics, J. Ceram. Soc. Jpn 104 (5) (1996) 462–465.
[12] H.H. Lu, J.L. Huang, Microstructure in silicon nitride containing β-phase seeding, J. Mater. Res. 14 (7) (1999) 2966–2973.
[13] S.Y. Lee, K.A. Appiagyei, H.D. Kim, Effect of β-Si_3N_4 seed crystal on the microstructure and mechanical properties of sintered reaction-bonded silicon nitride, J. Mater. Res. 14 (1) (1999) 178–184.
[14] Z. Javanovic, S. Kimura, O. Levenspiel, Effect of hydrogen and temperature on the kinetics of the fluidized-bed nitridation of silicon, J. Am. Ceram. Soc. 77 (1) (1994) 186–192.
[15] L.J. Gauckler, H. Hohnke, T.Y. Tien, The system Si_3N_4–SiO_2–Y_2O_3, J. Am. Ceram. Soc. 63 (1–2) (1980) 35–37.
[16] J.S. Lee, J.H. Mun, B.D. Han, D.S. Park and H.D. Kim, Effect of raw-Si particle size on the property of sintered reaction-bonded silicon nitride (to be submitted).